LONG-TERM PERFORMANCE OF EPOXY-COATED REINFORCING STEEL IN HEAVY SALT-CONTAMINATED CONCRETE

Seung-Kyoung Lee [1] and Y. Paul Virmani[2]

Abstract

This paper describes long-term natural weathering exposure testing of the remaining 31 post-Southern Exposure test slabs for the 1993–1998 Federal Highway Administration (FHWA) research project. When epoxy-coated reinforcing steel (ECRs) in the top mat coupled with the black bars in the bottom mat, the corrosion susceptibility was reduced to at least 50 percent of the black bar case. If top mat ECRs were connected to ECRs in the bottom mat, the mean macrocell current density was less than two percent of the highest black bar case even when ECRs contained defects, and approach the corrosion resistant level of stainless steel reinforcement.

Background

In May 1993, the Federal Highway Administration (FHWA) began a 5-year research project, *Corrosion Resistant Reinforcing for Concrete Components*. The objective of the study was to develop cost-effective new breeds of organic, inorganic, ceramic, and metallic coatings, as well as metallic alloys that could be utilized on or as reinforcement for embedment in portland cement concrete and ensure a corrosion-free design life of 75 to 100 years when exposed to adverse environments. The 1993–1998 research program involved testing of epoxy-coated, other polymer-coated, ceramic-coated, galvanized-clad, epoxy-coated galvanized-clad, stainless steel-clad, nickel-clad, copper-clad, corrosion resistance alloy-clad, inorganic silicate-clad, solid corrosion-resistance alloy steel, solid aluminum-bronze, solid stainless steels, and solid titanium reinforcing bars. Based on screening tests, the 141 reinforced concrete slab specimens using 12 different bar types were made and were exposed to the 96-week Southern Exposure (SE) testing. These tests were completed in late 1997, and the final report was published in a 1998 FHWA report, *Corrosion Evaluation of Epoxy-Coated, Metallic-Clad and Solid Metallic Reinforcing Bars in Concrete.* (McDonald, D.B., Pfeifer, D.W., and Sherman, M.R., 1998)

Configuration of the concrete slabs used in this FHWA study measured 30.5 x 30.5 x 17.8 cm (12 x 12 x 7 inches) and contained two layers of 29.2-cm (11.5-inch) long and 1.6-cm (5/8-inch) diameter reinforcement. The top mat acted as a macroanode and

[1] Research Corrosion Engineer, Federal Highway Administration, Turner-Fairbank Highway Research Center, Office of Infrastructure R & D

[2] Research Chemist, Federal Highway Administration, Turner-Fairbank Highway Research Center, Office of Infrastructure R & D

contained either two straight or two bent reinforcing bars, while the bottom mat was a macrocathode that contained four straight reinforcing bars. The top mat bar was connected to two bottom mat bars through a 10 Ω resistor. A clear cover of 2.5 cm (1.0 inch) was used in all specimens. While most previous published corrosion studies used only crack-free concrete slabs, some of the test slabs used in this project contained the cracks directly over a top mat rebar to simulate cracks observed on actual bridge decks.

The 96-week SE testing involved with the following wetting and drying cycles:

- Cyclic wetting and drying: 3-day drying at 38 °C (100 °F) and 60–80 percent relative humidity (RH), followed by 4-day ponding under a 15 percent NaCl solution at 16–27 °C (60–80 °F) for 12 weeks.
- Continuous ponding under a 15 percent NaCl solution at 16–27 °C (60–80 °F) and 60–80 percent RH for another 12 weeks.

The 15 percent salt solution was chosen to represent the high salt concentrations occurring on inland bridge structures from deicing salts. This 24-week cycle was repeated four times for a total test period of 96 weeks.

The ECR specimens in the 96-week SE test slabs were coated with six different powder coating products. The slabs were classified into four configuration groups. These were (1) slabs containing ECR in the top mat and black bar in the bottom mat (ECR top-black bottom, 19 slabs); (2) slabs containing ECRs in both mats (ECR top-ECR bottom, 6 slabs); (3) control slabs containing black bars in both mats (black top-black bottom, 3 slabs); and (4) slabs containing straight stainless steel bars coupled with either black or stainless steel bottom bars (stainless steel, 3 slabs). Among the 19 ECR top-black bottom slabs, 6 had two 180-degree bent ECRs in the top mat, and the concrete cover of another 7 slabs was precracked over the straight bars. One specimen of each black top-black bottom and stainless top-black bottom slabs contained 180-degree bent bars in the top mat. In addition, one black and stainless slab had precracks over the top mat bars. None of the ECR top-ECR bottom slabs contained bent bars or precracks. Every ECR bar was intentionally damaged by drilling holes through the coating to represent either 0.004 or 0.5 percent artificial coating defect using two different drill bit sizes. In every ECR top-ECR bottom slab, the two top mat ECRs contained different defect sizes, and a top mat ECR was paired with two bottom mat ECRs containing the same size of defect.

Experimental

After the conclusion of the 96-week SE testing in 1998, 31 post-SE test slabs that were not autopsied were then exposed to a long-term natural weathering at an outdoor test yard in Northbrook, IL, from September 1998 to December 2002. Corrosion progress of the top bar was monitored by short-circuit potential (SCP) and macrocell current. SCP was measured when top and bottom bars were electrically connected. On the other hand, macrocell current was measured as the voltage drop across a 10-Ω resistor connected between the top and bottom bar mats. The macrocell current data then were

converted into macrocell current density according to Ohm's law and a known surface area of 145.7 cm^2 (22.6 $in.^2$) for the anode (top bar). The same area was used for both coated and uncoated steel. Test data was collected periodically. During the last data measurements, additional data were collected, including the open-circuit potential (OCP) of top mat bars after the top and bottom mat bars were disconnected, the AC resistance between the top and bottom mats, and the impedance modulus ($|Z|$) at 0.1 Hertz (Hz) of top mat bars using Electrochemical Impedance Spectroscopy (EIS). Before autopsy, the exterior condition of the test slabs was documented using a digital camera.

When the test program ended after about 7 years, autopsy and subsequent laboratory analysis were performed with the test slabs, and the results are reported here. The tests include chlorides in the concrete, condition evaluation at bar/concrete interface, and visual examination of extracted bars. During the data analysis and autopsy, it was learned that macrocell current density was a good indicator of corrosion performance of the various reinforcements. Therefore, this article discusses corrosion performance of the test slabs, mainly in terms of macrocell current density data and autopsy results. For in-depth data analysis can be found in the report. (Lee, S.K. and Krauss, P.D., 2004)

Test Results and Discussion

1. Macrocell current and AC resistance

1.1 Test slabs containing black bars in both mats

Each of the black bar test slabs had cracking and delamination of the concrete cover after 96-week SE testing and before placing the slabs outdoors. Therefore, the macrocell currents measured after cracking are not indicative of the true difference in performance, because the corrosion rate drop after cracking and delamination of the concrete cover occurs. The straight, non-bent black bars had an average corrosion current density of about 2.4 $\mu A/cm^2$ (15.5 $\mu A/in.^2$) during the 96-week SE testing. Upon outdoor exposure, the black bar samples averaged somewhat less than 1.5 $\mu A/cm^2$ (9.7 $\mu A/in.^2$). This same effect may be present for some of the other poorly performing ECR samples with large damaged areas, precracks, and bending damage.

1.2 Test slabs containing ECRs in the top mat and black bars in the bottom mat

Test slabs containing ECRs performed better, especially the ones with smaller initial defect size (0.004 percent), than the black bar control slabs. Macrocell current density of the black bars became negative in every category after 1,600 days (see Figure 1). These negative current readings indicated reversal of macrocell current between original anode (top mat) and original cathode (bottom mat) at the time of measurement. Such current reversal was caused by corroding bottom mat cathode steel first instead of usual corrosion initiation at the top mat bars. This situation was possible when chloride

reached the black bars in the bottom mat and subsequently initiated the active corrosion there, while top mat ECRs were able to suppress corrosion. As discussed later, chloride concentration at some bottom bar depths was found to far exceed the chloride threshold for corrosion initiation of black bars (250 to 300 ppm).

1.3 Test slabs containing ECRs in both mats and stainless steel

Figure 2 shows variations of mean macrocell current density with time for the slabs containing either ECRs in both mats or stainless steel. There were three test slabs containing stainless steel bars in the top mat or in both mats, and two of them were precracked. Because of the small number of slabs, the stainless steel slabs were treated as one variable, even though some contained cracks and/or black bottom bars. Mean macrocell current density of stainless steel bars with black bottom steel became negative at around 1,600 days due to active corrosion in the bottom black mat.

When ECR was used in both mats in uncracked concrete, each pair of ECRs in the top and bottom mats contained the same coating damage (0.004 or 0.5 percent) and every slab contained two pairs of ECRs with each of the two coating defect areas. Mean macrocell current density data of the two mat ECR slabs were very small throughout the test period. The coating defect size did not make a noticeable difference in macrocell current density output, which approached that of stainless steel bars. This observation suggests that using ECRs in both mats in northern bridge decks is likely to give very high corrosion resistance in corrosive environments under deicing salt applications, and may approach an equivalent corrosion resistance to that offered by stainless steel bars.

1.4 Effect of bent ECR

When bent ECRs were connected to the black bottom bars, they produced the highest mean macrocell current density and were followed closely by the straight ECRs coupled with black bottom bars. In contrast, test slabs containing straight ECRs in both mats exhibited insignificant mean macrocell current density throughout the entire exposure period.

1.5 Further data analysis related to slab configuration and bar type

Figure 3 summarizes the macrocell current data according to four bar types (black, stainless steel, ECR with 0.5 percent initial coating damage, and ECR with 0.004 percent initial coating damage) and five slab configurations (straight top-black bottom-uncracked, straight top-ECR bottom-uncracked, straight top-black bottom-precracked, bent top-black bottom-uncracked, and stainless steel bars in uncracked). Mean macrocell current density varied significantly depending on slab configuration and bar type. The black bars produced the highest mean macrocell current density among various combinations of test variables regardless of slab configuration, i.e., presence of crack and bar shape (bent vs. straight). To illustrate relative significance of slab configuration and

bar type on the mean macrocell current density, Figure 4 presents the ratios of macrocell current density data shown in Figure 3 by dividing them by the highest average value (1.3 $\mu A/cm^2$ (8.4 $\mu A/in.^2$)) of the black bent bar-black bottom-uncracked concrete slabs. The stainless steel bars exhibited negligible mean macrocell current density which was only 1 percent of the highest black bar case. For straight ECRs, the mean macrocell current density was influenced by the size of the initial coating damage and whether the bottom mat bar was coated or uncoated. When straight ECRs in the top mat were coupled with black bars in the bottom mat, the size of coating defect became a factor for controlling macrocell current density. In the case of straight top ECRs containing 0.004 percent of initial coating defect coupled with black bottom bars, mean macrocell current density was 7 to 21 percent of the highest black bar case, depending on the presence of precracks. If straight top ECRs contained 0.5 percent initial coating defect, the current values increased to more than 40 percent of the highest black bar case, regardless of whether the slab had a precrack. For bent ECRs, even ones containing 0.004 percent coating damage produced noticeable macrocell current density when they were connected to black bottom bars, such that mean macrocell current density increased to 38 and 49 percent of the highest black bar case, regardless of initial coating defect size. If top mat ECRs were connected to ECRs in the bottom mats in uncracked concrete, the effect of coating damage on macrocell current density was minor, and the ratio decreased to no greater than 2 percent of the highest black bar data. They behaved similarly to stainless steel bars.

2. Statistical Analysis of Test Data

A statistical analysis was conducted to calculate sample mean ($\bar{x}$) and sample standard deviation (s) for macrocell current density. Then, the results were used to determine the 95 percent confidence interval for the unknown population mean (μ). The 95 percent confidence interval for μ means that researchers are 95 percent confident that the unknown μ is within this interval for a variable. Statistical analysis was performed for the variables classified by combinations of slab configuration and bar type.

Figure 5 shows distribution of μ's for the macrocell current density data categorized by 12 combinations of test variables. As noted in earlier sections, use of stainless steel bars and ECRs containing 0.004 percent initial coating damage produced the least current density. When ECRs having 0.5 percent initial coating defect are used in both mats, the macrocell current density slightly increased from zero. These are followed by straight ECRs containing 0.004 percent coating defects in the top mat only and other top mat only ECR cases. The black bar cases yielded the highest mean values.

3. Autopsy Results

Test slabs were split into several fragments by using a gas powered saw, a chisel and hammer. Embedded bars were then carefully extracted using a small chisel and hammer. Caution was exercised when removing ECRs to avoid coating damage. Figure

6 shows a photograph of a top mat straight ECR that performed well throughout the severe testing regime. The ECR and concrete/bar interface appearance was excellent, with no sign of corrosion. On the other hands, Figure 7 shows a severely corroded, straight, top mat ECR.

Closeup examination of the extracted ECRs revealed four different coating conditions, which are shown in Figure 8. When the ECR performed well, the exposed coating looked new with a glossy texture (Figure 8(a)). It was observed that when the epoxy coating reaches the advanced stage of deterioration due to corrosion, the coating exhibits numerous hairline cracks (Figure 8(b)) and then blisters (Figure 8(c)). Accumulation of multiple rust layers beneath disbonded coating was also a common corrosion morphology observed on severely corroded ECRs (Figure 8(d)). The disbonded coating mentioned above was defined as a permanently separated coating from substrate upon knife adhesion test performed several days after the ECRs were excavated. Therefore, it was different from temporary adhesion loss, which can recover fully or partially with time.

Figures 9 and 10 show photographs of autopsied bars taken after they were cleaned. The bars shown in Figure 9 were removed from slab #18, which contained ECRs in the top mat only. While one top ECR (the second bar from the top in the photograph) exhibited localized coating disbondment originated from corrosion at the smaller artificial coating defects (0.004 percent), the other top ECR (the first bar from the top in the photograph) experienced severe corrosion, again initiated at the larger artificial coating defects (0.5 percent), such that the epoxy coating could be peeled off completely. The bars shown in Figure 10 were removed from slab #10, which contained ECRs in both mats. While one top ECR (the second bar from top in the photograph) exhibited virtually no reduction in adhesion even at the smaller artificial coating defects (0.004 percent), the other top mat ECR (the first bar from top in the photograph) experienced moderate corrosion that initiated at the larger artificial coating defects (0.5 percent), such that epoxy coating could be peeled off locally around the initial defects. The ECRs extracted from the bottom mat were corrosion-free and had minimal adhesion loss.

4. Chloride Analysis

The experimental chloride data indicates that the water-soluble chloride concentration of the concrete is approximately 89 percent of the total (acid-soluble) chloride concentration. It was also noted that water-soluble chloride concentration in the top mat containing black bars was far lower than the rest. This is likely due to the fact that the slabs containing black bars were cracked and delaminated after the 96-week SE testing and before being placed outdoors. Rainwater passing through the cracks and delaminations likely dissolved some of the free chloride ions in the concrete near the top mat of steel. Compounding of the free chloride in the black bar rust products also may have occurred.

Conclusions

1. The black bars produced the highest mean macrocell current density among various combinations of test variables regardless of slab configuration, i.e., presence of crack and bar shape (bent vs. straight). The highest mean macrocell current density (1.3 $\mu A/cm^2$ (8.4 $\mu A/in.^2$)) was obtained from the black bent bar coupled with black bottom bars in uncracked concrete. In contrast, the stainless steel bars exhibited negligible mean macrocell current density, which was only 1 percent of the highest black bar case. Autopsy revealed that the corrosion morphology of black and stainless steel bars was consistent with the macrocell current density data. Macrocell current density was a good performance indicator of test slabs.

2. For straight top mat ECRs, the mean macrocell current density was influenced by the size of initial coating damage and type of bar in the bottom mat. When they were coupled with black bars in the bottom mat, the size of the coating defect became a critical factor for controlling macrocell current density. In the case of straight top mat ECRs containing 0.004 percent of initial coating defect coupled with black bottom bars, the mean macrocell current density was 7 to 21 percent of the highest black bar case, depending on whether the slab was precracked. If straight top mat ECRs containing 0.5 percent coating damage were connected to the black bottom bars, the current values increased to more than 40 percent of the black bar value, regardless of precracks in the concrete.

3. However, if straight ECRs in the top mat were connected to ECRs in the bottom mat in uncracked concrete, the mean macrocell current density decreased to no greater than 2 percent of the highest black bar case, regardless of the initial coating defect size. They behaved comparable to stainless steel bars.

4. Whenever an ECR slab with negligible macrocell current density was autopsied, the appearance of the ECR and concrete/bar interface was excellent with no sign of corrosion, and the coating looked new with a glossy texture. However, when severely corroded ECRs recognized by high macrocell current densities were autopsied, they revealed coating deterioration due to corrosion and exhibited numerous hairline cracks and/or blisters in conjunction with extensive coating disbondment and underlying steel corrosion. When test slabs exhibited severe damage, electrochemical test data collected from those slabs did not provide meaningful results.

5. Final defects were classified as bare area, mashed area (mechanical damage), coating crack, and holiday. Generally, the number of final coating defects on the autopsied ECRs increased from their initial values determined before embedment in concrete. This phenomenon was particularly pronounced for the poorly performing bars due to development of coating cracks, which was the most

frequent form of coating deterioration. Accumulation of multiple rust layers beneath disbonded coating is also a common corrosion morphology observed on severely corroded ECRs.

6. Reduced adhesion was usually initiated at the initial coating defects. It was much more pronounced on the top mat ECRs, irrespective of whether they were removed from ECR top-black bottom slabs or the ECR top-ECR bottom slabs, compared to those extracted from the bottom mat. The ECRs removed from the bottom mat also exhibited the lowest number of final defects and the strongest knife adhesion. No consistent trend was found between the level of macrocell current density and the extent of adhesion loss. Earlier FHWA studies investigated the coatings' adhesion using solution immersion tests and cathodic disbonding tests. (McDonald, D.B., Sherman, M.R., and Pfeifer, D.W., 1995, McDonald, D.B., Pfeifer, D.W., and Sherman, M.R., 1996, McDonald, D.B., Pfeifer, D.W., and Blake, G.T., 1996) Based on the review of the test results, the adhesion, as tested by solution immersion and cathodic disbonding tests, appeared to be a poor indicator of long-term performance of the coated bars in concrete. These findings suggest that there is no direct relationship between loss of adhesion and the effectiveness of ECR to mitigate corrosion.

7. According to impedance modulus, AC resistance, macrocell current density data, and autopsy results, the excellent performance of test slabs containing ECRs in both mats comparable to stainless steel bars may be attributed to the facts that electrical resistance was very high between the two ECR mats, and the ECRs in the bottom mat suppress the corrosion activity at the top mat ECR by minimizing the size of the available cathode.

8. This 7-year laboratory and outdoor exposure study confirmed that use of ECRs in the top mat only (uncoated bottom mat) reduced the corrosion susceptibility to at least 50 percent of the black bar case, even when the coating has damage. Hence, ECR used in the top mat alone would not provide optimum corrosion protection. If ECRs are used in both mats in uncracked concrete, corrosion resistance increases dramatically, even when the rebar coatings have defects. Such improved corrosion resistance can be attributed to a reduction in cathodic area (thus cathodic reaction), and higher electrical resistance between two mats of ECRs. This conclusion is valid even when they contain coating defects.

References

1. Lee, S.K. and Krauss, P.D., "*Long-Term Performance of Epoxy-Coated Reinforcing Steel in Heavy Salt-Contaminated Concrete*," Report No. FHWA-HRT-04-090, Federal Highway Administration, McLean, VA, May 2004.

2. McDonald, D.B., Sherman, M.R., and Pfeifer, D.W., *The Performance of Bendable and Nonbendable Organic Coatings for Reinforcing Bars in Solution and Cathodic Debonding Tests*, Report No. FHWA-RD-94-103, Federal Highway Administration, McLean, VA, January 1995.

3. McDonald, D.B., Sherman, M.R., and Pfeifer, D.W., *The Performance of Bendable and Nonbendable Organic Coatings for Reinforcing Bars in Solution and Cathodic Debonding Tests: Phase II Screening Tests*, Report No. FHWA-RD-96-021, Federal Highway Administration, McLean, VA, May 1996.

4. McDonald, D.B., Pfeifer, D.W., and Blake, G.T., *The Corrosion Performance of Inorganic-, Ceramic-, and Metallic-Clad Reinforcing Bars and Solid Metallic Reinforcing Bars in Accelerated Screening Tests*, Report No. FHWA-RD-96-085, Federal Highway Administration, McLean, VA, October 1996.

5. McDonald, D.B., Pfeifer, D.W., and Sherman, M.R., *Corrosion Evaluation of Epoxy-Coated, Metallic-Clad, and Solid Metallic Reinforcing Bars in Concrete*, Report No. FHWA-RD-98-153, Federal Highway Administration, McLean, VA, December 1998.

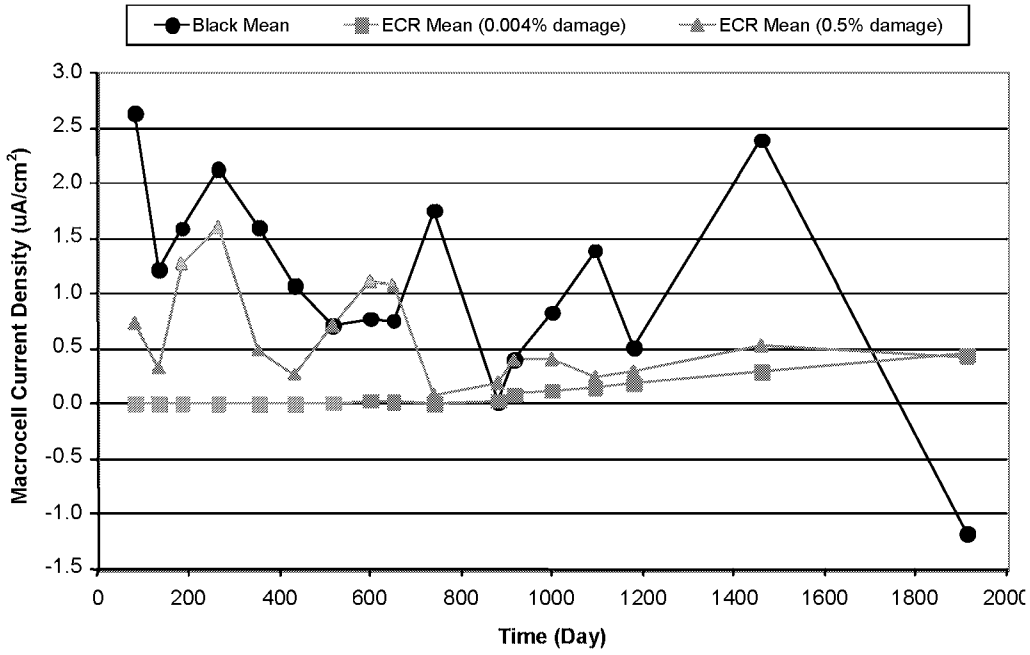

Figure 1. Macrocell current density change with time (straight top (black and ECR)-black bottom-uncracked concrete) during outdoor exposure

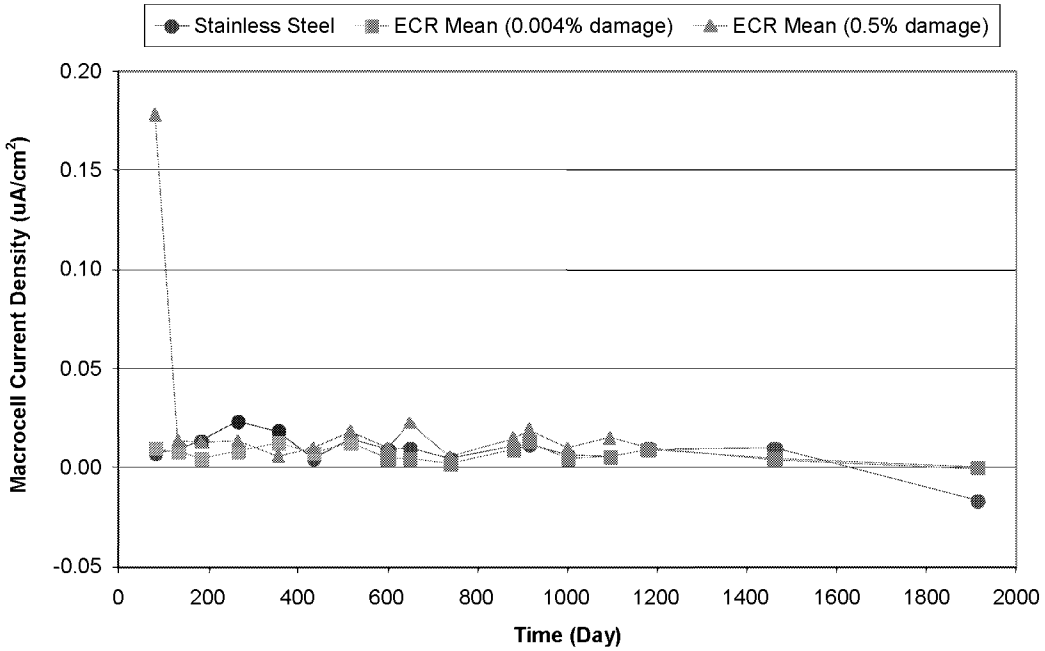

Figure 2. Macrocell current density change with time (stainless steel and ECR in both mats-uncracked concrete)

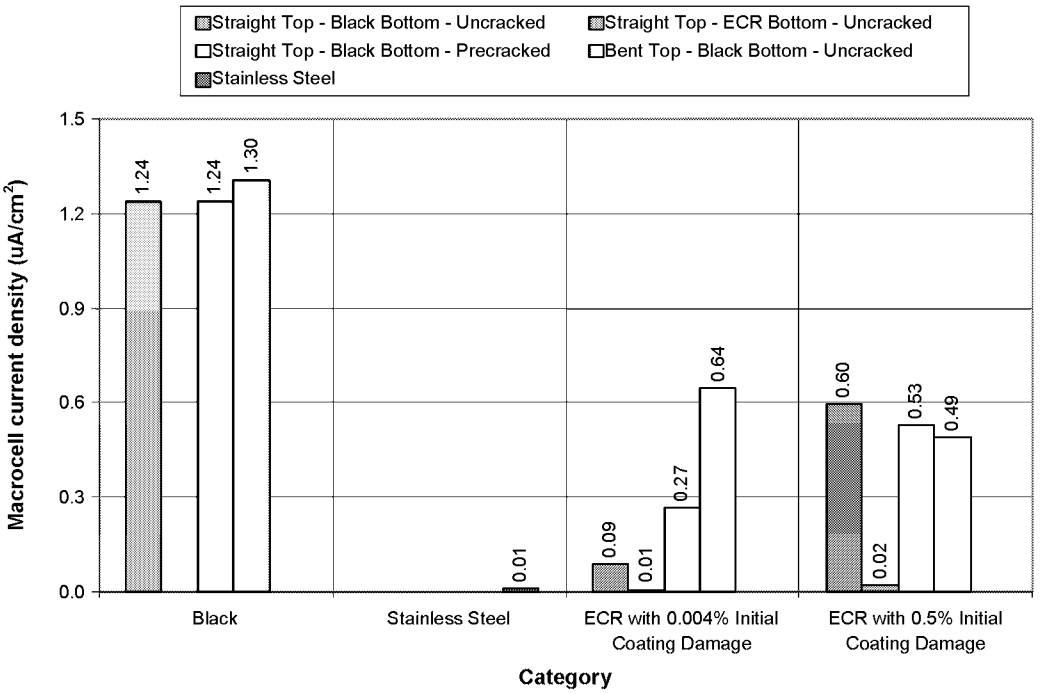

Figure 3. Mean macrocell current density data classified by bar type

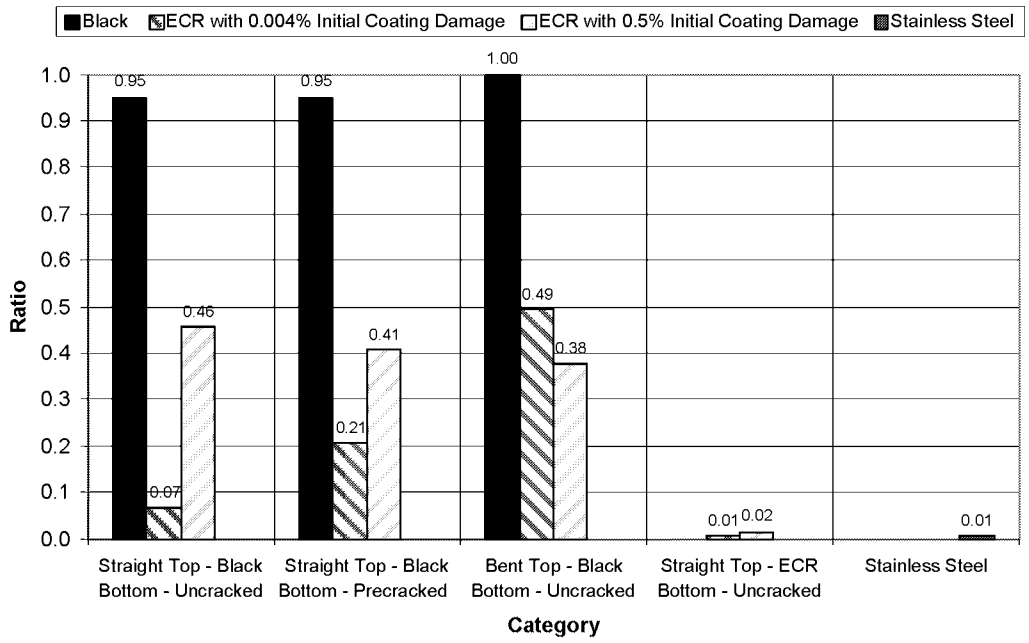

Figure 4. Relative ratio of macrocell current density per slab configuration

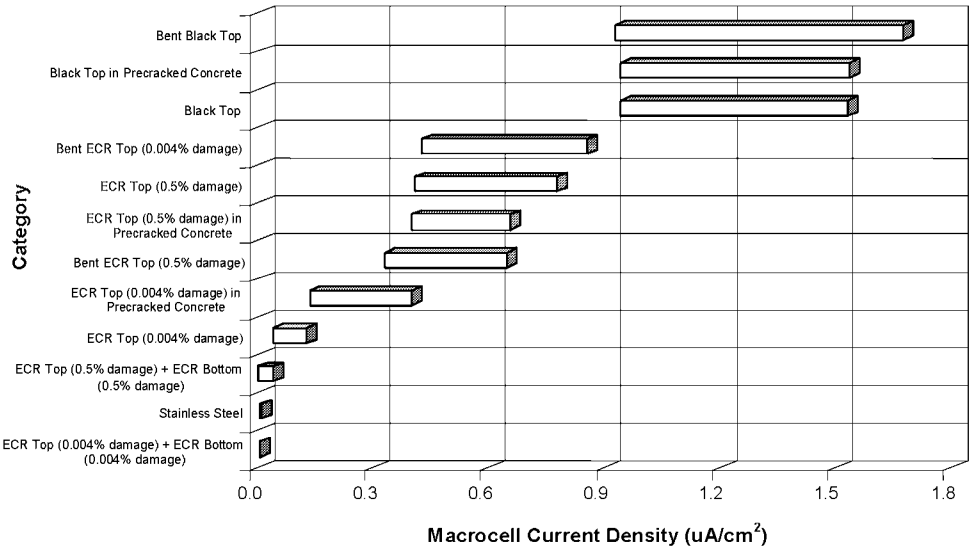

Figure 5. Ninety five percent confidence intervals for macrocell current density data

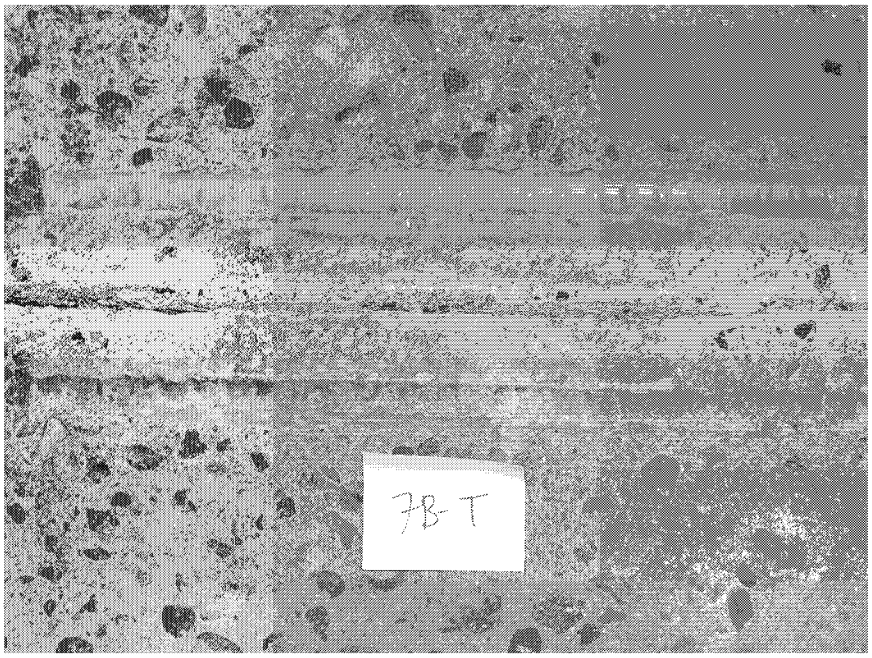

Figure 6. Typical condition of ECR with good corrosion resistance (slab #7—top right bar)

Figure 7. Typical condition of ECR with poor performance (slab #30—top right bar)

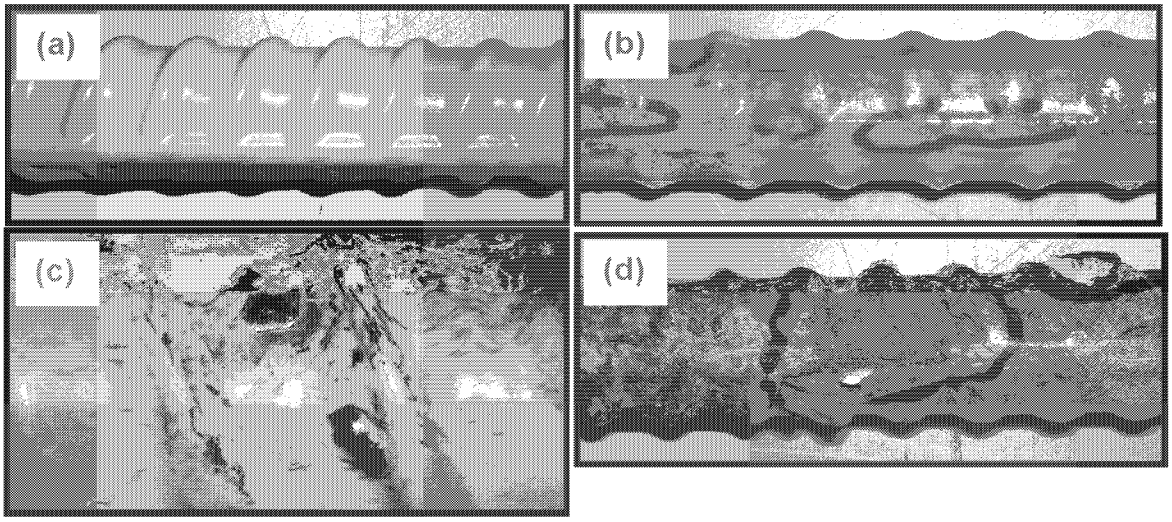

Figure 8. Closeup views of ECRs exhibiting various conditions: (a) an intact ECR; (b) an ECR containing hairline coating cracks; (c) an ECR containing coating blisters and hairline coating cracks; and (d) a delaminated ECR revealing severely corroded substrate

Figure 9. Photograph of autopsied bars extracted from slab #18 (ECR top-black bar bottom)

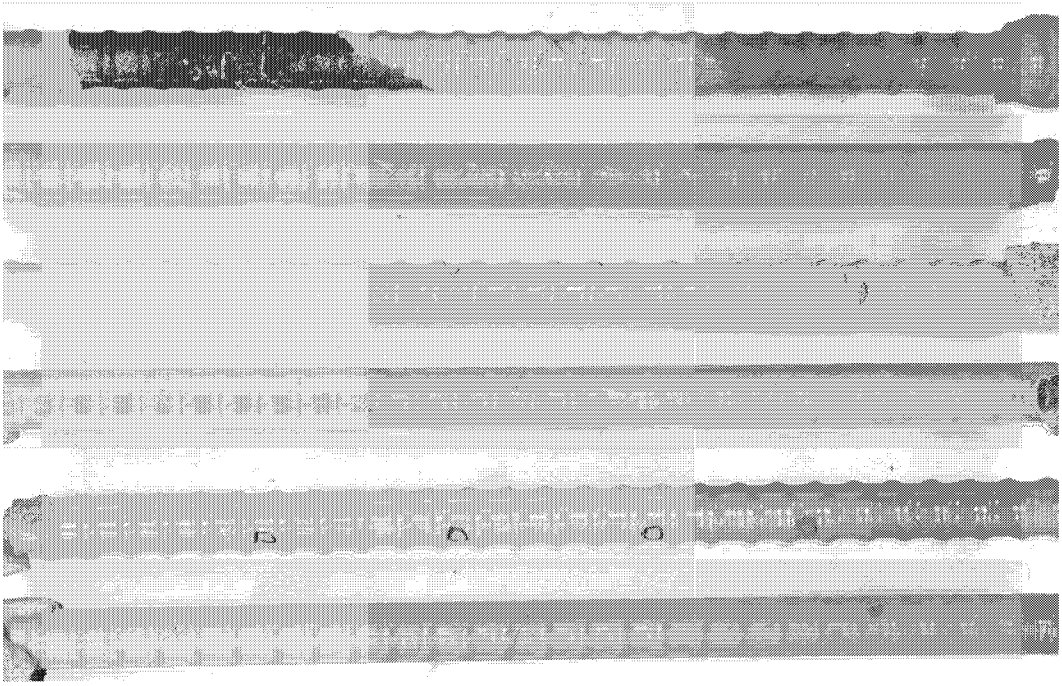

Figure 10. Photograph of autopsied bars extracted from slab #10 (ECRs in both mats)